

The diffuseness of low-mass galaxies in the FIREbox simulation

by
Marckie Zeender

Professor Moreno, Advisor

A thesis submitted in partial fulfillment
of the requirements for the
Degree of Bachelor of Arts with Honors
in Physics



Claremont, California
April 13, 2023

Abstract

This thesis examines the variance in the size-mass ratio for low-mass satellite galaxies within the FIREbox simulation. To find possible causes for this variance, I defined a diffuseness parameter for galaxies which represents this deviation. I calculated the distribution of this parameter for both FIREbox and the Local Group. For FIREbox galaxies, I further compared the parameter with a galaxy's proximity to its host galaxy, its minimum proximity, and the distance to its nearest neighbor. I found that above a critical threshold of $\approx \frac{1}{5}$ of the host's Virial radius, there was a significant negative correlation between diffuseness and minimum proximity. This implies that the variance in diffuseness is partially caused by tidal interactions with other galaxies.

Executive Summary

Cosmological simulations are an important part of our understanding of the universe. They allow us to test our theories about cosmology by seeing if the simulated behavior created by those theories aligns with the real world. The FIREbox galaxy simulation uses the theory of Λ CDM, the current most popular model of dark matter and dark energy. It models a box of over 1700 galaxies from their initial creation all the way through the present day. This present day state can be compared to real world galaxies to determine what simulated characteristics align with the real ones.

When a certain characteristic of the simulation does not line up with observational data, it is called a **tension**. One such tension is that of the diversity of low-mass galaxy sizes. The low-mass galaxies near the Milky Way (known as the **Local Group**) have much variation in radius compared to their mass. In other words, they range from very compact to very diffuse. However, most historical simulated galaxies have a much stricter size-mass ratio. This discrepancy is the driving motivation for this thesis.

To examine this tension further, I compare the diffuseness of galaxies in FIREbox with other galactic properties. I define the **diffuseness** (β) of a galaxy to be how much it deviates from the expected size-mass ratio. This parameter is useful for our study because, by design, it is independent of mass for low-mass galaxies. We are therefore free to correlate it with other parameters.

One theory for the variation in diffuseness is tidal interactions. A tidal interaction occurs when a galaxy comes in close contact with another, and its outer layers get stretched by the other's gravity. Tidal forces therefore could cause greater diffuseness. Satellite galaxies are ones that orbit other galaxies. By examining the relationship between a satellite and its host galaxy, one may find the potential effects of tidal forces on galaxy diffuseness. I compared the diffuseness of satellite galaxies with the distance to their hosts: both in the present and when it was at its minimum distance. I found that when one expresses the distance as a fraction of the host galaxy's virial radius, there is a correlation. Specifically, the closer a satellite gets to its host, the more diffuse it becomes. I also examined the relationship between a galaxy and its nearest neighbor. There is a similar negative correlation.

We can therefore conclude that tidal forces play a role in modifying the diffuseness

of galaxies, although there are likely other important factors as well. More research will need to be put into what may contribute to the very wide range of diffuseness in the Local Group.

Acknowledgments

I dedicate this to my good friend Ben Getchell. Your mind could move galaxies.

I am writing this while standing on the backs of giants. Thank you to my wonderful partner Maggie, who has been at my side throughout this entire process; from helping me with statistics to moral support to getting me water, I could not have done this without you. Thank you to my suitemates and to all my friends, you have stuck with me through late nights and long uncommunicative periods. Thank you to my mom, dad, and sister for supporting me in my lifelong dream to study astrophysics, and for sending me to this school. Thank you to the Pomona college faculty and staff; they work tirelessly to ensure the success and wellbeing of us students. A special thanks to Professor Whitaker, my academic advisor and the physics department chair; you make this department what it is and it shows.

And last but certainly not least, thank you to Professor Moreno. Through the good and the bad, the over-enthusiasm and the debilitating anxiety, you have been so supportive and understanding. It has been my pleasure and my honor work with you this year. I could not have asked for a better project, nor for a better thesis advisor.

Contents

Abstract	i
Executive Summary	ii
Acknowledgments	iv
1 Introduction	1
1.1 Physical models	1
1.2 Low-mass galaxies and their tensions	3
1.3 Tension in the size-mass relation	3
2 Methods	5
2.1 FIREbox: a novel cosmological simulation	5
2.2 The data	5
2.3 The Diffuseness Parameter	7
2.4 Proximity	10
2.4.1 Minimum Proximity	10
3 Results and discussion	11
3.1 Diversity of low-mass galaxy diffuseness	11
3.2 Proximity to host galaxy	11
3.3 Minimum proximity	12
3.4 Proximity to nearest neighbor	14
4 Conclusions and future work	15
4.1 Size-mass-proximity relation	15
4.2 Further Work	16
4.3 Closing Remarks	16
A Calculating distances in FIREbox	19

List of Figures

- | | | |
|-----|--|---|
| 1.1 | From: nasa.gov. A real-world example of gravitational lensing. In the center is an elliptical galaxy (yellow). The blue ring, known as an Einstein Ring, is actually another galaxy that lies behind the first one. It is visually distorted into a ring shape by the gravitational lensing of the yellow galaxy. Without dark matter (or a competing theory), the lensing effect would be much weaker. | 2 |
| 1.2 | From: Sales et al. (2022). A comparison of the sizes and masses of low-mass galaxies from simulations and reality. The y axis plots r_{50} and the x axis plots M_{50} . The gray squares depict real galaxies from the Milky Way's local group, whose data was compiled by McConnachie (2012). The other colors depict data from various simulations other than FIREbox. As we can see, the dwarfs from the local group show much diversity in their size-mass ratios. The simulated galaxies, however, show more consistency, especially when compared to others from their own simulation (for example, notice that the orange circles are all clustered together). This paper will extend this analysis to the FIREbox data. | 4 |
| 2.1 | A comparison the size and detail of cosmological simulations. There is a tradeoff between scale and resolution, where a total increase in both means a higher dynamic range at the cost of computer performance. FIREbox has the highest dynamic range, and therefore the highest computational cost. | 6 |
| 2.2 | From: Feldmann et al. (2022). A representation of the FIREbox simulation. The first two rows depict the state of the simulation at three different time points; the rightmost images depict the simulation in the present time. The top row depicts dark matter in blue and stellar matter in white, while the middle row depicts gas. The bottom row shows a galaxy at different scales within a cluster. As we can see, matter collects into galaxies and systems of galaxies over the course of the simulated universe's evolution. These galaxies take on a variety of sizes, and they share threads of gas and are contained within hierarchical halos of dark matter. | 8 |

2.3	The left shows the size-mass relationship for the FIREbox low-mass galaxies. It covers the range $3 \cdot 10^3 - 10^9$. Galaxies larger than this are no longer dwarfs and do not follow the power law, and galaxies smaller than this approach FIREbox's resolution limit. The line of best fit is described by equation 2.3 and β represents the deviation from that line. β is chosen to characterize the diffuseness of a galaxy because the distribution of β is essentially independent of mass, which can be seen in on the right.	9
3.1	Shows the diffuseness of satellites as a function of distance to their host galaxies. On the left, it compares the absolute separation. On the right, it shows the Virial separation (distance as a fraction of the host galaxy's Virial radius). The correlation for these is small: $r = .22, p \leq .001$ for d and $r = .26, p \leq .001$ for d/R_{vir} . This slight positive correlation in both sets of parameters is likely caused by the dark matter deficient galaxies (shown in light green and yellow), whose outer regions are likely tidally disrupted, leaving only a core.	12
3.2	Shows the diffuseness of satellites as a function of minimum distance to their host galaxies. On the left, it compares the absolute separation. On the right, it shows the Virial separation. There is no correlation for these parameters: $r = .04, p = .51$ for d_{min} and $r = -0.07, p = .25$ for d_{min}/R_{vir}	13
3.3	A zoom-in of figure 3.2 showing the diffuseness of satellite galaxies as a function of their minimum Virial separation. This graph only includes galaxies above the critical separation of $0.2R_{vir}$, below which a galaxy would either be entirely destroyed or converted into a dark matter deficient galaxy. There is a medium negative correlation between these parameters: $r = -0.32, p \leq .001$	13
3.4	Shows a galaxy's distance to its nearest neighbor. There is a slight negative correlation between these parameters: $r = .26, p \leq .001$. This result shows that the tidal disruption hypothesis could be extended beyond just satellite galaxies.	14

Chapter 1

Introduction

Understanding the composition and structure of galaxies, and the role that dark matter plays in their organization, is a pressing topic in modern cosmology. A common method to explore these questions is with numerical simulations. This approach allows us to choose plausible initial conditions and laws of physics in order to test how the universe would behave. We can then compare those results to real-world observations to determine the accuracy of those physical assumptions, and we can predict new effects that can be confirmed by observations. For instance, if we wanted to test Newton’s theory of gravity in our solar system, we could run a numerical simulation of Newton’s equation using a known initial position of the planets, and test whether the simulated motion of the planets aligns with reality. Likewise, we can test our theories about dark matter and gravity by running cosmological simulations. These simulate a space full of stars, gas, and dark matter that evolves into a system of galaxies.

1.1 Physical models

Our current leading theory for dark matter’s role in galaxy evolution is the cosmological constant plus cold dark matter (Λ CDM) model (White and Rees, 1978). This theory provides a framework for cosmological simulations that incorporates a non-interacting model for dark matter and the cosmological constant model of dark energy. The “cold” dark matter model means that we assume that dark matter particles interact with neither each other nor “normal” baryonic matter, except through gravity. This is in contrast to other competing theories such as superfluid dark matter, which interacts with itself to form a superfluid (De Luca and Khouri, 2023). These dark matter models predict large dark matter halos around galaxies (Feldmann et al., 2022). Such predictions are consistent with our observations of gravitational lensing—visual distortions due to gravity. They also are a better (though imperfect) fit for the rotation curves of galaxies—the orbital velocity of stars as a function of their distance to their galaxy’s center Sales et al. (2022). Not much is known about dark matter beyond its gravitational effects on baryonic matter, and we have yet to

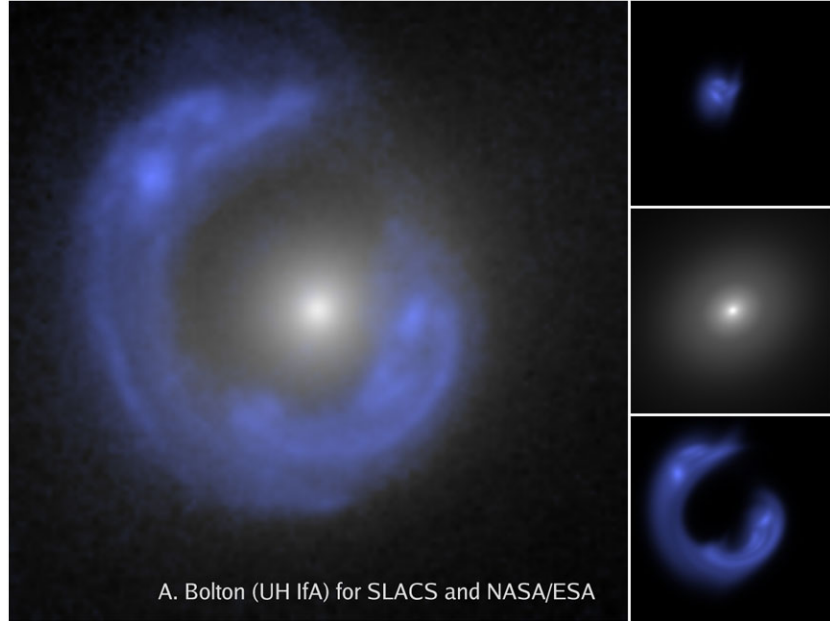


Figure 1.1: From: nasa.gov. A real-world example of gravitational lensing. In the center is an elliptical galaxy (yellow). The blue ring, known as an Einstein Ring, is actually another galaxy that lies behind the first one. It is visually distorted into a ring shape by the gravitational lensing of the yellow galaxy. Without dark matter (or a competing theory), the lensing effect would be much weaker.

discover a non-gravitational interaction between these two.

The Λ CDM paradigm assumes dark energy to be the cosmological constant Λ , which is a degree of freedom in the Einstein Equation that adds a net offset to the energy density of a vacuum. However, there are alternative theories of dark energy; Bassi et al. (2023) shows that the Bimetric gravity model could also explain the effects of dark energy. If more evidence can be found in support of these alternative models, then Bimetric and/or superfluid dark matter may replace Λ CDM as the leading cosmological model.

When creating a cosmological simulation, astrophysicists must also incorporate baryonic processes, the physics of ordinary matter. These processes include chemistry, thermal physics, and the formation, evolution, and feedback of stars. Our current computers limit us such that we cannot resolve individual stars within galaxies (Feldmann et al., 2022) because they are simply too small, and stellar physics at these scales is not fully understood. Earlier simulations, such as Bournaud et al. (2010), were forced to ignore stellar processes entirely in favor of gaseous ones. They found that the simulated galaxies grew too massive and cooled too quickly compared to real galaxies. This tension was resolved by the creation of the “Feedback in Realistic Environments” (FIRE) physics model (Hopkins et al., 2018). FIRE adopts a subgrid model that simulates large chunks of matter (referred to as particles), each containing many stars. It then uses the estimated number of stars in each particle to

simulate stellar feedback.

1.2 Low-mass galaxies and their tensions

As telescopes have improved, we have had an increase in observations of low-mass “dwarf” galaxies. Before this, the Λ CDM model was questioned because it predicted the existence of many more low-mass galaxies than had been observed in the region around the Milky Way (Klypin et al., 1999). According to Sales et al. (2022), enough low-mass galaxies have been discovered in recent years to resolve this tension. However, the sudden influx of low-mass galaxy observations has provided astrophysicists number of new tensions. The diversity of the size-mass relation of low-mass galaxies is one such tension. Observational data of low-mass galaxies near the Milky Way suggests that the correlation between the mass and size of satellite low-mass galaxies is not as strong as simulations seem to predict (Sales et al., 2022).

1.3 Tension in the size-mass relation

The observed low-mass galaxies near the Milky Way have widely varying radii compared to their masses. In other words, both diffuse and compact low-mass galaxies are relatively common. However, zoom-in galaxy simulations, including Fitts et al. (2017), tend to form galaxies with much stricter size-mass ratios (Sales et al., 2022). Some may argue that these discrepancies are caused by numerical inaccuracy. However, even the simulations with the highest numerical resolution such as Wheeler et al. (2019) lack diversity in size-mass ratios for low-mass galaxies.

The diversity of sizes of low-mass galaxies must therefore be caused by something else. Tidal disruption could be the answer. When a low-mass galaxy passes by a larger galaxy, its dark matter halo can be destroyed by the tidal force exerted on it, according to Moreno et al. (2022). This can also lead to the creation of an ultra-compact low-mass (Applebaum et al., 2021), because the galaxy will lose its outer regions. It is therefore plausible that close interactions between galaxies is what causes variance in size.

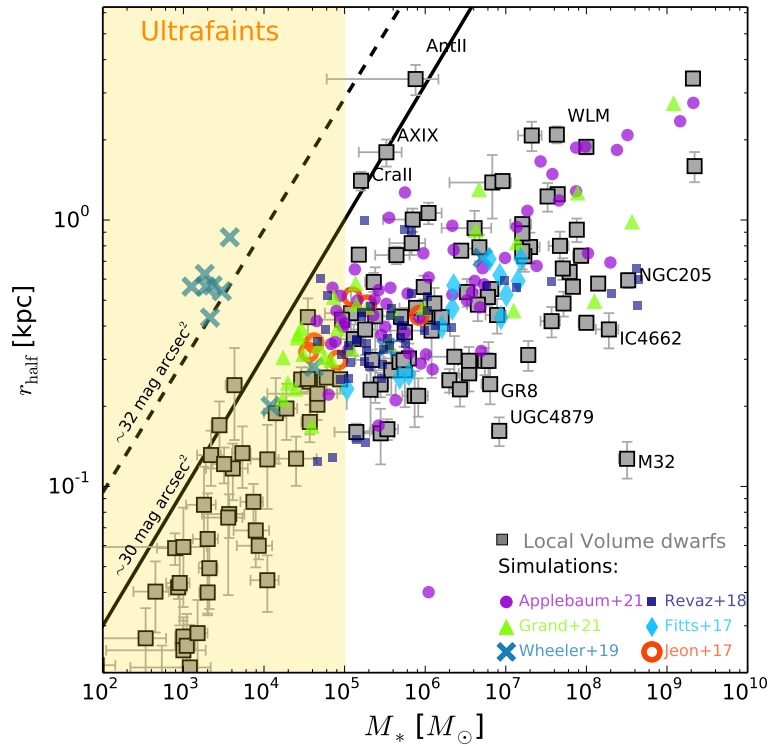


Figure 1.2: From: Sales et al. (2022). A comparison of the sizes and masses of low-mass galaxies from simulations and reality. The y axis plots r_{50} and the x axis plots M_{50} . The gray squares depict real galaxies from the Milky Way's local group, whose data was compiled by McConnachie (2012). The other colors depict data from various simulations other than FIREbox. As we can see, the dwarfs from the local group show much diversity in their size-mass ratios. The simulated galaxies, however, show more consistency, especially when compared to others from their own simulation (for example, notice that the orange circles are all clustered together). This paper will extend this analysis to the FIREbox data.

Chapter 2

Methods

2.1 FIREbox: a novel cosmological simulation

Scale and resolution are important for simulations. Astrophysicists must balance large volume and high detail, both of which cost computing power. The large volume simulations allow us to closely study intergalactic systems and to collect large amounts of statistical information about galaxies (Feldmann et al., 2022). However, a higher resolution “zoom in” simulation such as FIRE in the Field (Fitts et al., 2017) allows us to better simulate the internal physics of the galaxies themselves.

This paper will examine data from FIREbox (Feldmann et al., 2022). This cosmological simulation does not have the largest volume, nor is it the most detailed. Rather, it incorporates a balance of high detail and large scale (see figure 2.1), which together give it the highest dynamical range of any cosmological simulation to this date.

2.2 The data

Over the course of the evolution of the FIREbox simulation, 1201 snapshots of the state of the universe were collected (Feldmann et al., 2022). They were approximately evenly spaced out in time and included the positions of the particles, their densities, metallicities, star-formation rates, and other properties. The particle data was reduced by grouping the particles into their respective galaxies and dark matter halos. They used the AMIGA Halo Finder (AHF; Knollmann and Knebe (2009)) to sort the halos into categories of halos and sub-halos, which in turn allowed them to categorize the galaxies by host and satellite galaxies respectively. The reduced data, known as the galaxy and halo catalog, includes galaxy information such as position, radius, mass and star formation rate, as well as data about the dark matter halos around those galaxies. For the extent of this experiment, we will be using the snapshot 1201, the final state of the simulation. This snapshot depicts the simulated present day.

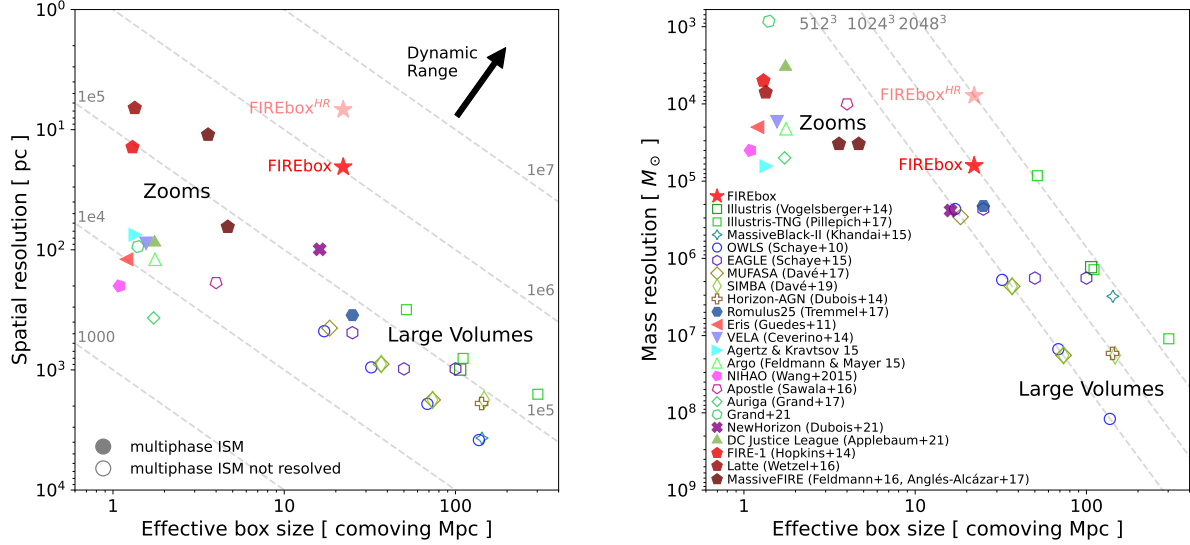


Figure 2.1: A comparison the size and detail of cosmological simulations. There is a tradeoff between scale and resolution, where a total increase in both means a higher dynamic range at the cost of computer performance. FIREbox has the highest dynamic range, and therefore the highest computational cost.

Each parameter for the galaxies is split between a few different definitions. For the purpose of this experiment, we will use the following definitions unless otherwise specified. The galaxy's radius R_{50} is defined to be the radius that contains 50% of its stars, as determined by AHF. The galaxy's mass M_* is defined to be the mass of the stars contained within R_{50} . We are not going to include dark matter in this definition. The reader should note that this is not the only way to define these parameters. Due to the fluid nature of matter on a galactic scale, it is often arbitrary as to whether a given particle belongs to a given galaxy. Alternate definitions include different thresholds for the radius, such as R_{80} , and different kinds of matter included in the mass, such as gas matter and dark matter.

Other parameters that we will use are a galaxy's position in space and its flyby distance—a satellite galaxy's minimum distance to its host galaxy. All distances (including radius) are measured in terms of the co-moving parameter h , a time-dependent scaling factor of the universe. In the final state of FIREbox, $h = 0.6774\text{kpc}$.

McConnachie (2012) compiled a number of data sets for low-mass galaxies in the local group of the Milky Way. One data set includes the galaxies' radii and another contains their mass. The radius is defined slightly differently in this case. It is the half-light radius, the radius from which half of the galaxy's light is emitted. The mass parameter is calculated by assuming a mass-light ratio of one, meaning that the brightness per unit mass is equal to the Sun. For the sake of this experiment, we will assume that the half-light radius is equal

to R_{50} the presumed M_* is equal to M_* . To get this data in a usable form, I first dumped the text-based datasets into pandas spreadsheets. I removed invalid rows and then merged them by galaxy name. For galaxies whose names were reported differently on the different sheets, I merged them by hand. I then cast the mass and radius to float64 for use in the analysis.

2.3 The Diffuseness Parameter

As diffuseness will be main subject of this paper, let us define it. The low-mass galaxies in FIREbox loosely follow a power law size-mass relationship (see figure 2.3). The relationship can therefore be described using the following equation.

$$\frac{R_{50}}{1kpc} \approx a \left(\frac{M_*}{M_\odot} \right)^\gamma \quad (2.1)$$

Where γ and a are constants and M_\odot is the mass of the sun. We are dividing by a kiloparsec unit to make the equation unitless. Taking the logarithm of this equation gives us

$$\ln \left(\frac{R_{50}}{1kpc} \right) \approx \ln(a) + \gamma \ln \left(\frac{M_*}{M_\odot} \right) \quad (2.2)$$

By taking the logarithm of a power law, we end up with an equation for a line. This linear relationship can be seen in figure 2.3. $\ln(a)$ becomes the y-intercept of the line and γ becomes the slope. We have kept denoting this equation as *approximately* equal in order to emphasize that not every galaxy falls exactly into this relationship. However, we can replace that by introducing a galaxy-specific parameter β that is defined to be the galaxy's deviation from this linear relationship.

$$\ln \left(\frac{R_{50}}{1kpc} \right) = \ln(a) + \gamma \ln \left(\frac{M_*}{M_\odot} \right) + \beta \quad (2.3)$$

$$\beta \equiv \ln \left(\frac{R_{50}}{1kpc} \right) - \ln(a) - \gamma \ln \left(\frac{M_*}{M_\odot} \right) \quad (2.4)$$

We will call β the **diffuseness parameter**, because it tells us how diffuse a galaxy is relative to its fellow galaxies. Positive values of β mean that the galaxy has a larger radius than other galaxies of the same mass, and negative values mean a smaller radius. β

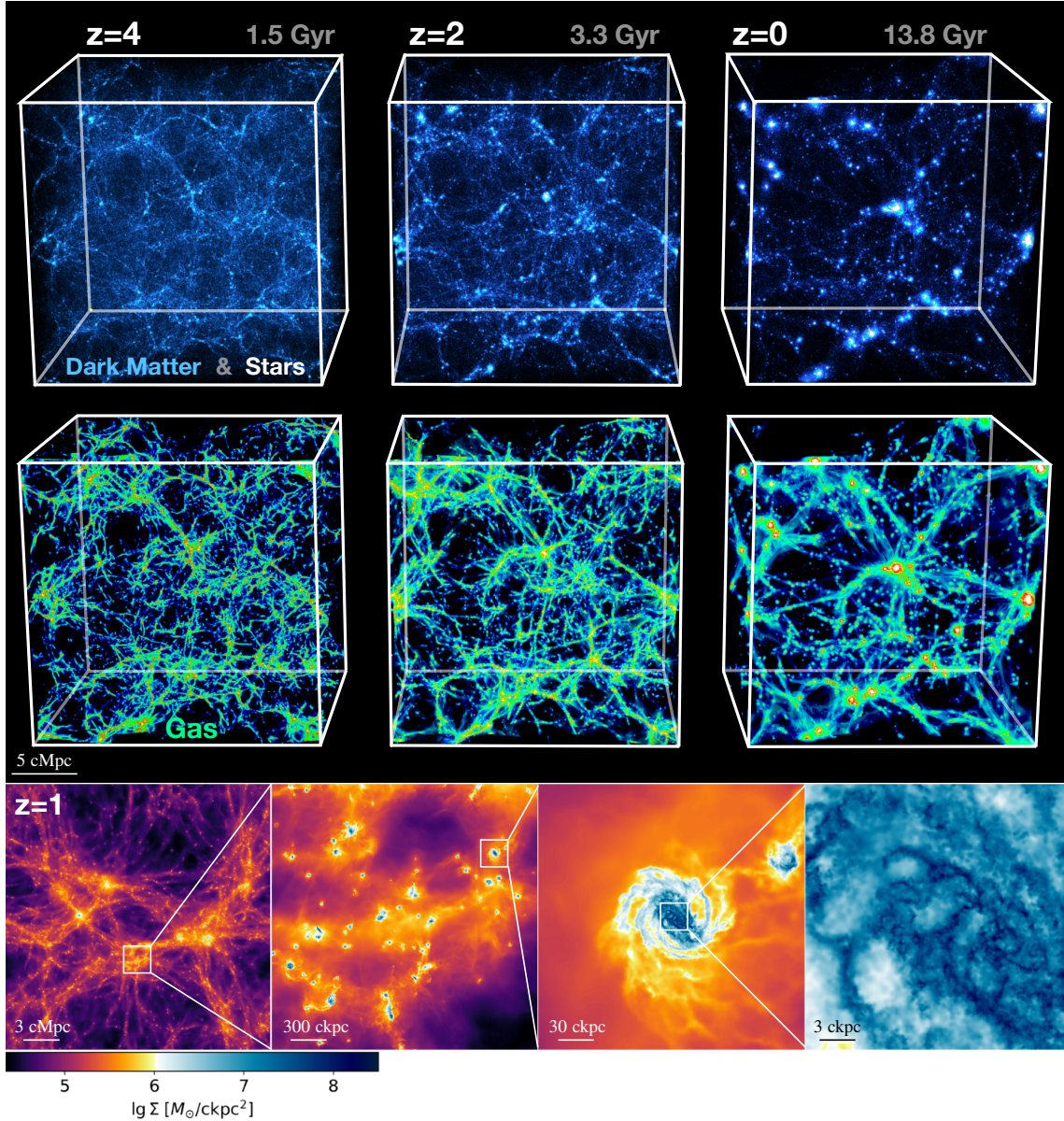
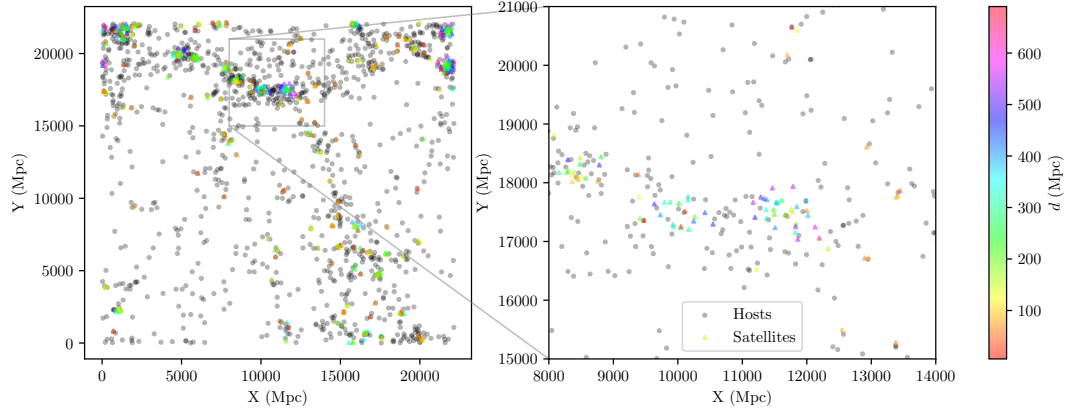


Figure 2.2: From: Feldmann et al. (2022). A representation of the FIREbox simulation. The first two rows depict the state of the simulation at three different time points; the rightmost images depict the simulation in the present time. The top row depicts dark matter in blue and stellar matter in white, while the middle row depicts gas. The bottom row shows a galaxy at different scales within a cluster. As we can see, matter collects into galaxies and systems of galaxies over the course of the simulated universe's evolution. These galaxies take on a variety of sizes, and they share threads of gas and are contained within hierarchical halos of dark matter.



A 2D visualization of FIREbox; the X and Y coordinates of each galaxy. Host galaxies are depicted as gray circles, and satellites galaxies are triangles that are colored by the distance to their host galaxy.

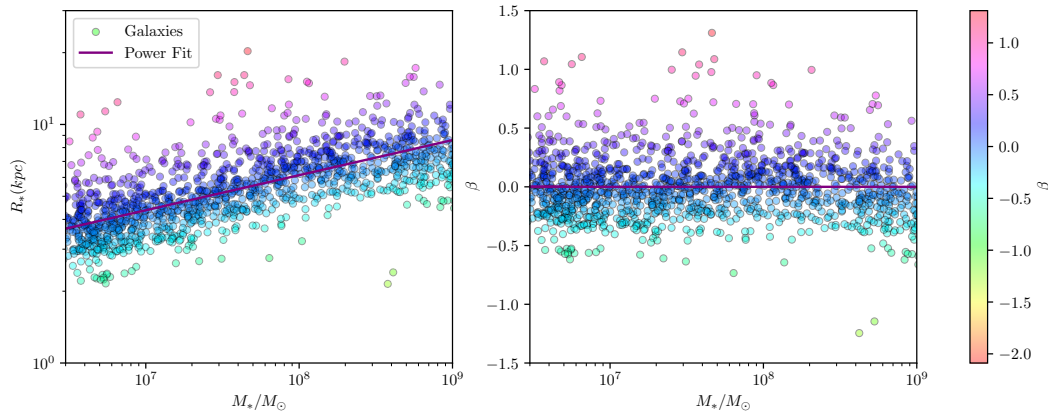


Figure 2.3: The left shows the size-mass relationship for the FIREbox low-mass galaxies. It covers the range $3 \cdot 10^3 - 10^9$. Galaxies larger than this are no longer dwarfs and do not follow the power law, and galaxies smaller than this approach FIREbox's resolution limit. The line of best fit is described by equation 2.3 and β represents the deviation from that line. β is chosen to characterize the diffuseness of a galaxy because the distribution of β is essentially independent of mass, which can be seen in on the right.

is especially useful for characterizing the diffuseness because the distribution of β remains consistent across all masses of low-mass galaxies (see figure 2.3). Note that this does not apply for galaxies larger than $10^9 M_\odot$, as they stop following the power law.

We can calculate γ and $\ln(a)$ using equation 2.3 and fitting the dataset to a line. We can then use those values in equation 2.3 to find each galaxy's value of β . We can also characterize the **diversity of the diffuseness** of galaxies using the standard deviation σ_β (the mean is zero by design). We will use these values to compare FIREbox with the galaxies of the Local Group.

2.4 Proximity

To determine what may cause differences in the diffuseness of galaxies, one thing that we may look at is its interactions with its neighbors. Specifically, we will examine a galaxy's distance to its nearest neighbor as well as a satellite galaxy's distance to its host galaxy (as defined by AHF). For the distance to the host galaxy, I examined both the absolute separation and virial separation. I define the absolute separation to be the distance in kpc to the host galaxy, and the virial separation to be that distance as a fraction of the host galaxy's virial radius. The virial radius of a galaxy is the radius within which particles will tend to be gravitationally bound. In other words, it is the effective radius of a galaxy's gravitational well.

Calculating the distance between two galaxies is not as trivial as it may seem because of the shape of FIREbox. The simulation volume is defined as a cube that repeats itself (Feldmann et al., 2022). In other words, if you travel across one border of the universe you appear on the opposite side. This is done to avoid any strange boundary conditions from affecting the simulation, but also without having to simulate an infinite region. In order to measure the X component of the distance between two objects one must first determine whether they are across the X border. If they are, then we find the sum of the distances to the border. Otherwise, we find the difference of their positions like normal. The same logic is used to find the Y and Z components. Only then do we calculate magnitude of the distance. Refer to Appendix A for code to do this calculation.

2.4.1 Minimum Proximity

To determine whether tidal interactions affect the diffuseness of galaxies, it is better to look at the *minimum* distance between a satellite and its host, as opposed to the current distance. The minimum distance is the point at which the tidal forces are strongest, and therefore could cause the most extreme effects. We must therefore also compare β to d_{min} .

Chapter 3

Results and discussion

3.1 Diversity of low-mass galaxy diffuseness

There are only so many conclusions we can draw about the diversity of low-mass galaxy sizes with the given data. The data from McConnachie (2012) spans the range of 10^2 to 10^9 solar masses, with many of the galaxies observed being smaller than $3 \cdot 10^6$. The FIREbox data, however, only covers galaxies greater than $3 \cdot 10^6$. For this reason and others, the lines of best fit defined by $\ln(a)$ and γ (see equation 2.3) for each dataset do not perfectly line up. The diffuseness parameter β is defined relative to the line of best fit for a dataset. It is therefore important to note that the β for individual galaxies across datasets have no meaningful comparison. However, we may still compare the overall diversity of the diffuseness. For FIREbox we have $\sigma_\beta = 0.28$, and for McConnachie (2012) we have a diversity of $\sigma_\beta = 0.66$, over twice as large. The simulated galaxies in FIREbox therefore follow a much stricter size-mass relationship than is expected from real-world observation.

This discrepancy is an example of the diversity of low-mass galaxy sizes tension, and Sales et al. (2022) has already shown that it applies to many higher resolution simulations. FIREbox has a larger volume and contains more galaxies than those simulations, and is the first of its size to be detailed enough to resolve low-mass galaxies. It is therefore an important finding that the tension is not resolved in FIREbox, because that is evidence that the tension is *not* caused by a constraint in simulation volume.

3.2 Proximity to host galaxy

We find that there is a small correlation between (the logarithm of) a satellite's distance to its host galaxy and its diffuseness (see figure 3.1). This correlation is approximately the same regardless of whether we measure the absolute separation or Virial separation: $r = .22$, $p \leq .001$ for the former and $r = .26$, $p \leq .001$ for the latter. As we can see in the figures, the

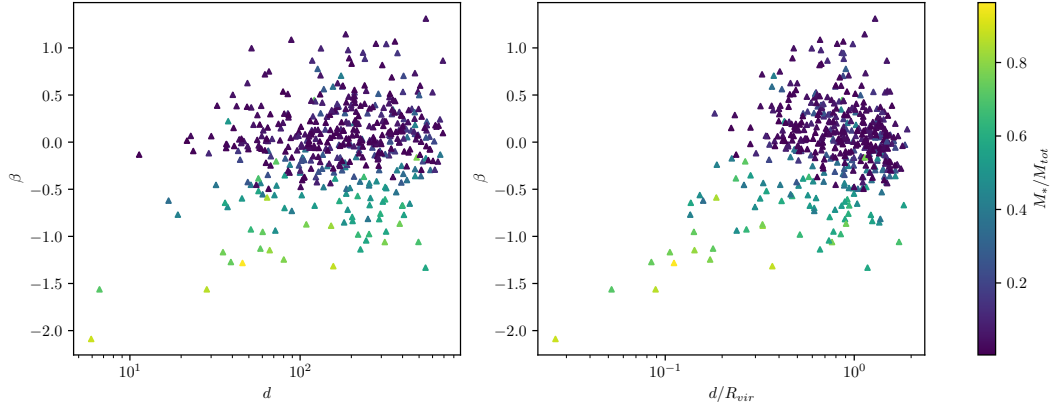


Figure 3.1: Shows the diffuseness of satellites as a function of distance to their host galaxies. On the left, it compares the absolute separation. On the right, it shows the Virial separation (distance as a fraction of the host galaxy’s Virial radius). The correlation for these is small: $r = .22, p \leq .001$ for d and $r = .26, p \leq .001$ for d/R_{vir} . This slight positive correlation in both sets of parameters is likely caused by the dark matter deficient galaxies (shown in light green and yellow), whose outer regions are likely tidally disrupted, leaving only a core.

data is essentially untouched except for the galaxies of low dark matter with $d/R_{vir} < 0.2$. Below this threshold, as Moreno et al. (2022) establishes, a satellite galaxy experiences a level of tidal disruption that either disassembles it entirely forms a dark matter deficient galaxy. However, above this threshold there appears to not be much of an effect. In fact, if we exclude galaxies below this critical threshold from our analysis, we find that there is absolutely no correlation: $r = .06, p = .23$ for absolute distance and $r = -.03, p = .51$ for Virial separation. We may therefore conclude that a variance in proximity to a host galaxy is not responsible for the diversity of diffuseness in galaxies.

3.3 Minimum proximity

When we plot the diffuseness of a satellite against the minimum separation between it and its host, we find an uneven distribution (see figure 3.2). A majority of galaxies are clustered towards the right, and only a few outliers are towards the bottom left. However, we notice that these outliers are the dark matter deficient galaxies. Including the outliers gives us no correlation for these parameters: $r = .04, p = .51$ for d and $r = -.07, p = .25$ for d_{min}/R_{vir} .

However when we exclude galaxies with $d_{min} \leq 0.2R_{vir}$, we get a much different picture. While there is no correlation for the absolute distances ($r = -0.03, p = .62$) there is a medium negative correlation between β and d_{min}/R_{vir} : $r = -0.32, p \leq .001$.

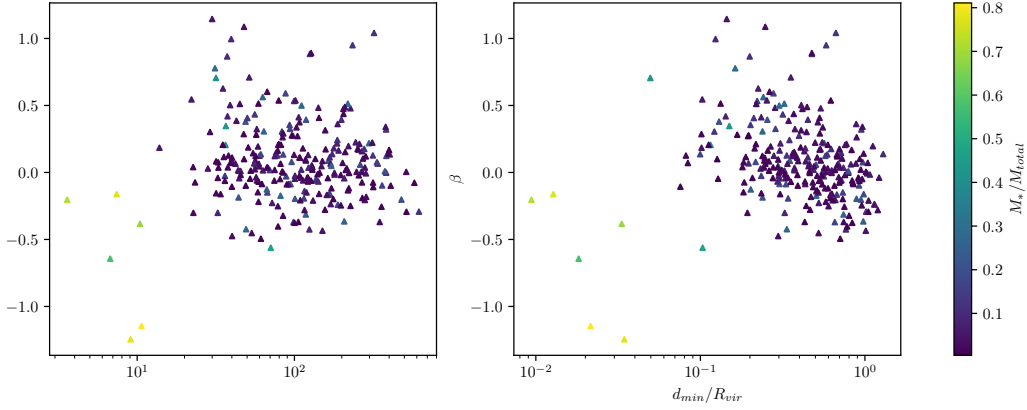


Figure 3.2: Shows the diffuseness of satellites as a function of minimum distance to their host galaxies. On the left, it compares the absolute separation. On the right, it shows the Virial separation. There is no correlation for these parameters: $r = .04$, $p = .51$ for d_{min} and $r = -0.07$, $p = .25$ for d_{min}/R_{vir} .

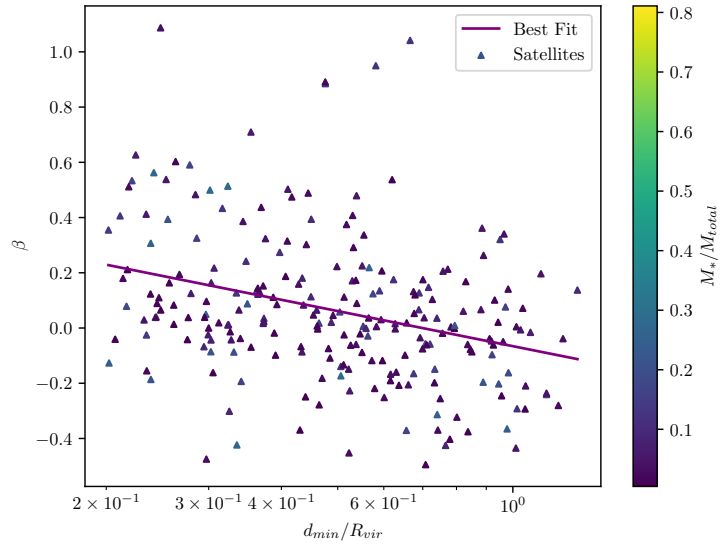


Figure 3.3: A zoom-in of figure 3.2 showing the diffuseness of satellite galaxies as a function of their minimum Virial separation. This graph only includes galaxies above the critical separation of $0.2R_{vir}$, below which a galaxy would either be entirely destroyed or converted into a dark matter deficient galaxy. There is a medium negative correlation between these parameters: $r = -0.32$, $p \leq .001$

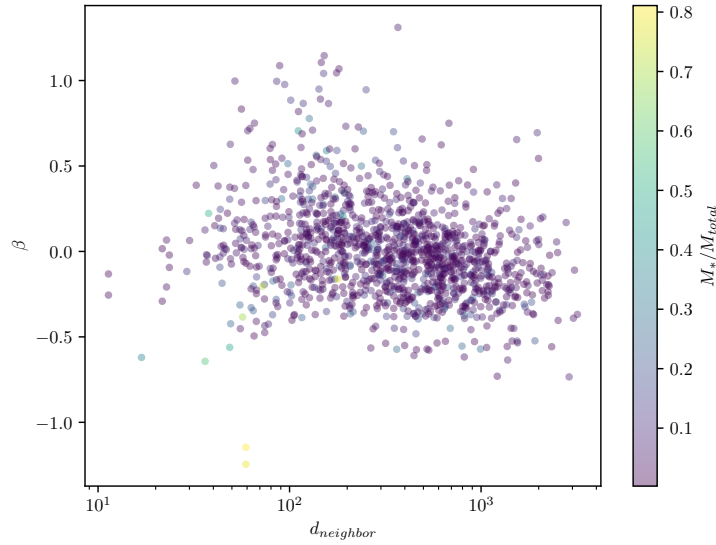


Figure 3.4: Shows a galaxy's distance to its nearest neighbor. There is a slight negative correlation between these parameters: $r = .26, p \leq .001$. This result shows that the tidal disruption hypothesis could be extended beyond just satellite galaxies.

3.4 Proximity to nearest neighbor

Plotting the proximity of a galaxy to its nearest neighbor gives a similar graph, with a slightly smaller correlation: $r = .26, p \leq .001$. There is again a slight negative trend, with the primary outliers being dark matter diffuse galaxies.

Chapter 4

Conclusions and future work

4.1 Size-mass-proximity relation

We discovered that β is correlation with the log of a satellite's proximity to its host galaxy. This relationship, as we will demonstrate, implies that we can include this distance as a new term in the formula for the size-mass relationship (equation 2.3). To prove this, we will reverse engineer that equation starting from equation 2.3. We will begin by expressing β in terms of d_{min}/R_{vir} using the experimental results found in figure 3.3.

$$\beta = -0.18 \ln \left(\frac{d_{min}}{R_{vir}} \right) \quad (4.1)$$

Where -0.18 is the slope of the line of best fit in this relationship. We can plug this into equation 2.3, giving us

$$\ln \left(\frac{R_{50}}{1kpc} \right) = \ln(a) + \gamma \ln \left(\frac{M_*}{M_\odot} \right) - 0.18 \ln \left(\frac{d_{min}}{R_{vir}} \right) \quad (4.2)$$

We take the exponent to reveal the final power law relationship.

$$R_{50} = a \left(\frac{M_*}{M_\odot} \right)^\gamma \left(\frac{d_{min}}{R_{vir}} \right)^{-0.18} kpc \quad (4.3)$$

And finally, we may plug in the experimental values of a and γ (see figure 2.3). This gives us a final equation of

$$R_{50} = 0.41 \left(\frac{M_*}{M_\odot} \right)^{0.15} \left(\frac{d_{min}}{R_{vir}} \right)^{-0.18} \text{ kpc} \quad (4.4)$$

As we can see, a satellite's distance to its host has just as much of an influence on its radius as its mass does.

4.2 Further Work

If you compare figure 3.1 and 3.2, you will notice a number of blue-ish datapoints that exist in only the former. They do not appear in the latter graph because there was no minimum distance data for them. Their blue color-coding indicates that they have lower amounts of dark matter ($M_*/M_{tot} \approx 0.6$). Additionally, they fall noticeably lower on the plot than their purple neighbors, indicating that they tend to be more compact. These galaxies likely hold an important piece of the puzzle to finding the causes of variance in diffuseness for galaxies, as well as their dark matter content. Further work should focus on these galaxies, including investigating the reason why they are considered to not have a minimum distance to their host galaxy.

This thesis covers correlations in the FIREbox data. However, it is clear from our calculation of σ_β for the Local Group that the real world holds a much greater range of diffuseness values than even FIREbox. There could be many explanations for this. Firstly, there could be some mechanism causing the tidal effects to be even more pronounced than the simulations suggest. Secondly, the higher diffuseness diversity could be caused by a higher diversity in distances between galaxies. Thirdly, there could be other variables contributing to the diffuseness. And finally, the tension could still be evidence that Λ CDM is wrong. Further work should pursue these topics.

My results show results for proximity to a galaxy's nearest neighbor. However, given that many satellite galaxies orbit their nearest neighbor, d is not orthogonal to $d_{neighbor}$. Future research should control for this to determine whether the tidal effects in a host-satellite relationship are different from those of arbitrary interactions between neighboring galaxies.

4.3 Closing Remarks

We have found that tidal interactions play a role in creating diffuse galaxies. Be it a satellite that is orbiting close to its host galaxy or simply a stray galaxy passing another, its size can be forever changed by this interaction. There are likely many undiscovered methods by which a galaxy's diffuseness can evolve over time, some of which may not be present in FIREbox, but the confirmation of tidal effects brings us one step closer to understanding the nature of low-mass galaxies.

Bibliography

- L. V. Sales, A. Wetzel, and A. Fattahi, *Nature Astronomy* **6**, 897 (2022), ISSN 2397-3366.
- A. W. McConnachie, *The Astronomical Journal* **144**, 4 (2012), ISSN 1538-3881.
- R. Feldmann, E. Quataert, C.-A. Faucher-Giguère, P. F. Hopkins, O. Çatmabacak, D. Kereš, L. Bassini, M. Bernardini, J. S. Bullock, E. Cenci, et al., *FIREbox: Simulating galaxies at high dynamic range in a cosmological volume* (2022), [arXiv:2205.15325](https://arxiv.org/abs/2205.15325).
- S. D. M. White and M. J. Rees, *Monthly Notices of the Royal Astronomical Society* **183**, 341 (1978), ISSN 0035-8711.
- V. De Luca and J. Khouri, *Superfluid Dark Matter around Black Holes* (2023), [arXiv:2302.10286](https://arxiv.org/abs/2302.10286).
- A. Bassi, S. A. Adil, M. P. Rajvanshi, and A. A. Sen, *Cosmological Evolution in Bimetric Gravity: Observational Constraints and LSS Signatures* (2023), [arXiv:2301.11000](https://arxiv.org/abs/2301.11000).
- F. Bournaud, B. G. Elmegreen, R. Teyssier, D. L. Block, and I. Puerari, *Monthly Notices of the Royal Astronomical Society* **409**, 1088 (2010), ISSN 0035-8711.
- P. F. Hopkins, A. Wetzel, D. Kereš, C.-A. Faucher-Giguère, E. Quataert, M. Boylan-Kolchin, N. Murray, C. C. Hayward, S. Garrison-Kimmel, C. Hummels, et al., *Monthly Notices of the Royal Astronomical Society* **480**, 800 (2018), ISSN 0035-8711.
- A. A. Klypin, A. V. Kravtsov, O. Valenzuela, and F. Prada, *The Astrophysical Journal* **522**, 82 (1999), ISSN 0004-637X, 1538-4357, [astro-ph/9901240](https://arxiv.org/abs/astro-ph/9901240).
- A. Fitts, M. Boylan-Kolchin, O. D. Elbert, J. S. Bullock, P. F. Hopkins, J. Oñorbe, A. Wetzel, C. Wheeler, C.-A. Faucher-Giguère, D. Kereš, et al., *Monthly Notices of the Royal Astronomical Society* **471**, 3547 (2017), ISSN 0035-8711.
- C. Wheeler, P. F. Hopkins, A. B. Pace, S. Garrison-Kimmel, M. Boylan-Kolchin, A. Wetzel, J. S. Bullock, D. Kereš, C.-A. Faucher-Giguère, and E. Quataert, *Monthly Notices of the Royal Astronomical Society* **490**, 4447 (2019), ISSN 0035-8711.

- J. Moreno, S. Danieli, J. S. Bullock, R. Feldmann, P. F. Hopkins, O. Catmabacak, A. Gurvich, A. Lazar, C. Klein, C. B. Hummels, et al., *Nature Astronomy* **6**, 496 (2022), ISSN 2397-3366, 2202.05836.
- E. Applebaum, A. M. Brooks, C. R. Christensen, F. Munshi, T. R. Quinn, S. Shen, and M. Tremmel, *The Astrophysical Journal* **906**, 96 (2021), ISSN 0004-637X.
- S. R. Knollmann and A. Knebe, *The Astrophysical Journal Supplement Series* **182**, 608 (2009), ISSN 0067-0049.

Appendix A

Calculating distances in FIREbox

The following code finds the distance to the closest galaxy. Note that for each coordinate, one must check whether the separation is greater than 7500, implying that the distance should be measured across the border.

```
def get_nearest(row):

    r = np.array([
        row.Xc_ahf_cat, row.Yc_ahf_cat, row.Zc_ahf_cat
    ]).reshape((1, 3))

    r_other: np.ndarray = dat.loc[:, (
        'Xc_ahf_cat', 'Yc_ahf_cat', 'Zc_ahf_cat'
    )].to_numpy(dtype='float64')

    # 2d array: each row contains the x, y, z separation
    delta_r_vec = r_other - r

    # whether the coordinate is across the border
    is_over = delta_r_vec > 7500

    # if across the border, subtract delta_r from 15000
    delta_r_wrapped = (15000 - delta_r_vec) * is_over

    # else, use delta_r as is.
    delta_r_wrapped += delta_r_vec * ~is_over

    # find the magnitude
    delta_r_mag = np.sqrt((delta_r_wrapped ** 2).sum(axis=1))
```

```
delta_r_mag += 15000 * (delta_r_mag == 0.0)

nearest_galaxy = dat[ 'galaxyID' ].to_numpy( dtype=int )[ delta_r_mag . argmin ()]

prox_to_nearest = delta_r_mag . min()

return pd . Series (
    dict (
        galaxyID=row . galaxyID ,
        nearest_galaxy=nearest_galaxy ,
        d_comoving=prox_to_nearest ,

        rvir_nearest=dat[ 'Rvir_ahf_cat' ].to_numpy(
            dtype='float64'
        )[ delta_r_mag . argmin ()]
    )
)
```